slight base line drifts are still seen in these chromatograms. Temperature programming requires much shorter reconditioning time than solvent gradient elution. This is another advantage of the temperature programming.

Cooling effluents is important not only to prevent base line drift but also to enhance the sensitivity of the conductometric detection. This detection is based on the POE complex formation with alkali-metal ions in the mobile phases; smaller mobility of the complex results in the negative conductometric response (*9*). The complex formation of POEs is also an exothermic process, and high temperature impedes the complex formation and lowers the sensitivity. Hence, the detection at lower temperature is essentially important to obtain higher sensitivity.

In conclusion, the present temperature programming has some advantages over solvent gradient elution for analyses of POEs: (1) it can be performed with simple instruments; (2) it permits the use of bulk-solution detectors; (3) a very short time is required to recondition the column for the repeated analyses. However, the present method simultaneously has the following disadvantages: (1) reproducibility is poorer than when thermostated systems are employed; (2) the exponential temperature gradient made difficult the theoretical prediction of the retention.

ACKNOWLEDGMENT

I thank Tosoh Co. for generous gifts of the separation columns.

LITERATURE CITED

(1) Snyder, L. R. *J. Chromatogr.* **1979**, *179*, 167-172.
(2) Melander, W. R.; Chen, B.-K.; Horváth, C. *J. Chromatogr.* **1979**, *185*, 99-109.
(3) Melander, W. R.; Nahum, A.; Horváth, C. *J. Chromatogr.* **1979**, *185*, 129-152.
(4) Bowermaster, J.; McNair, H. *J. Chromatogr.* **1983**, *279*, 431-438.
(5) Melander, W. R.; Chen, B.-K.; Horváth, C. *J. Chromatogr.* **1985**, *318*, 1-10.
(6) Carr, P. W.; Doherty, R. M.; Kamlet, M. J.; Taft, R. W.; Melander, W.; Horváth, C. *Anal. Chem.* **1986**, *58*, 2674-2680.
(7) Carr, J. W.; Harris, J. M. *J. Chromatogr.* **1989**, *481*, 135-146.
(8) Okada, T. *Anal. Chem.* **1990**, *62*, 327-341.
(9) Okada, T. *Anal. Chem.* **1990**, *62*, 734-738.
(10) Okada, T. *Macromolecules*, **1990**, *23*, 4216-4219.
(11) Hirata, Y.; Sumiya, E. *J. Chromatogr.* **1983**, *267*, 125-131.
(12) Jinno, K.; Phillips, J. B.; Carney, D. P. *Anal. Chem.* **1985**, *57*, 574-576.
(13) Biggs, W. R.; Fetzer, J. C. *J. Chromatogr.* **1986**, *351*, 313-322.
(14) McCown, S. M.; Southern, D.; Morrison, B. E.; Garteiz, D. *J. Chromatgr.* **1986**, *352*, 483-492.
(15) Shintani, H.; Dasgupta, P. K. *Anal. Chem.* **1987**, *59*, 802-808.
(16) Cross, J. In *Nonionic Surfactants*; Cross, J., Ed.; Dekker: New York, 1987; p 3.
(17) Vögtle, F.; Weber, E. *Angew. Chem. Int. Ed. Engl.* **1979**, *18*, 753-776.
(18) Krstulovic, A. M.; Brown, P. R. *Reversed-Phase High Performance Liquid Chromatography*; Wiley: New York, 1982.
(19) Pohl, C. A.; Johnson, E. L. *J. Chromatogr. Sci.* **1980**, *18*, 442-452.

RECEIVED for review December 4, 1990. Accepted February 25, 1991.

CORRESPONDENCE

Scanning Tunneling Microscopy and Atomic Force Microscopy in the Characterization of Activated Graphite Electrodes

Sir: To date there have been many methods described to activate carbon electrodes, including electrochemical treatment (*1-17*), laser irradiation (*18-21*), radio-frequency (RF) plasma (*22*), and heat treatment (*23-26*). These methods were developed empirically, and only now is an understanding of parameters controlling surface activity beginning to emerge (*20, 27*). Electrochemical treatment and laser irradiation are particularly attractive treatments because they are relatively inexpensive, are quick, and can be performed without removing the electrode from solution. Activation, common to these procedures, may be attributable to an increase in the exposed edge plane density, which has been associated with faster kinetics (*14, 20*). Copper deposition in conjunction with scanning electron microscopy (SEM) has shown an increase in the density of localized defects on active surfaces (*15*); an increase in surface activity is associated with an increase in the density of the localized defects (*15*). Scanning tunneling microscopy (STM), phase detection microscopy, and SEM have also been used to study the effects of electrochemical treatment of highly oriented pyrolytic graphite (HOPG) (*13*) and glassy carbon (GC) (*16, 17*). These studies have suggested an increase in surface roughness consistent with an increase in the density of exposed edge planes.

An additional effect of the electrochemical treatment of GC and HOPG is the formation of an oxide layer (*5, 11, 13*). The amorphous nature of graphite oxide and its uneven distribution over the electrode surface (*13*) may result in an electronically inhomogeneous surface. In a case where a surface is electronically inhomogeneous, changes in tunneling current can be a result of changes in topography and/or in local electronic structure (*28*). As a result, STM images may provide misleading information about the topography.

Atomic force microscopy (AFM) has been shown to be effective in studies of the topography of both conducting and insulating surfaces because it does not require the sample to be conducting (*29, 30*). As a result, AFM should not be affected by local changes in electronic structure. For this reason, AFM was used in conjunction with STM to study the effect of electrooxidative activation of GC.

EXPERIMENTAL SECTION

Reagents. All solutions were made with deionized/distilled water. Reagent-grade sodium phosphate monobasic and dibasic and potassium nitrate were obtained from Baker. Sulfuric acid and potassium chloride were obtained from Fisher and MCB, respectively. All reagents were used as received.

Electrode Preparation. Electrodes consisted of 3-mm-diameter GC-10 (Electrosynthesis), which were sealed in glass with Torr-Seal epoxy (Varian Associates). Electrodes were resurfaced with 5-, 0.3-, and finally 0.05-μm alumina on microcloths by using a polishing wheel (Buehler) (*4*). The electrodes were finally ultrasonicated for 5 min in distilled water. Electrochemical treatment was achieved by poising a polished GC electrode at +1.8

0003-2700/91/0363-1047$02.50/0

V for 5 min followed by −0.1 V for 2 min in 0.1 M supporting electrolyte (2). Electrochemically treated electrodes were rinsed with copious amounts of distilled water and were allowed to dry under ambient conditions for 24 h.

Electrochemical treatment was performed with a Bioanalytical Systems BAS-100 analyzer and an electrochemical cell with a Ag/AgCl reference electrode and a Pt wire auxiliary electrode. All solutions were deaerated with nitrogen for 5 min prior to experiments.

STM and AFM Conditions. STM and AFM were performed in air by using a Nanoscope II (Digital Instruments). Both STM and AFM images were generated by maintaining a constant signal (current and force, respectively) between the tip and the sample. This was achieved by controlling the potential applied to a calibrated piezo element in a feedback circuit. Pt–Ir (80/20) Nanotips, used to obtain STM images, were used as received. STM images were obtained in the constant current mode with a tunneling current of 2 nA, a tip bias of +100 mV, and a scan rate of 40 Hz. To ensure that the STM tips were free from contamination, HOPG was intermittently imaged with atomic resolution.

AFM studies were performed in the constant force mode, using 100-μm Si_3N_4 triangular cantilevers with a spring constant of 0.58 N/m at a scan rate of 20 Hz. This results in a constant force between 1 and 100 nN being applied to the sample. All AFM images produced by this method were stable while continuously scanning the surface, suggesting that the surface was not being damaged as a result of rastering the tip across the surface.

The images presented here are representative of many images taken at different points on each sample. All STM and AFM images were low pass filtered to remove high-frequency noise which did not alter the topographical heights (27).

RESULTS AND DISCUSSION

The electrochemical oxidation of graphite has been studied extensively (31). At low supporting electrolyte concentrations (less than 1 M) and low graphite crystallinity, intercalation efficiency is low (32, 33). As a result, side reactions including oxidation of water, production of surface oxides, and corrosion of the surface become more dominant. Graphite oxide formation has been reported in neutral or acid supporting electrolytes with oxygen-containing anions (5, 11, 34). In contrast, the formation of graphite oxide in supporting electrolytes containing chloride salts is reported to be much less efficient (34). This is a result of the oxidation of chloride, which occurs more readily than the oxidation of the electrode surface.

Supporting electrolytes consisting of 0.1 M KNO_3, NaH_2PO_4/Na_2HPO_4, H_2SO_4, and KCl were chosen to determine the effect of electrochemical treatment on the surface structure of GC. Figure 1 shows the result of electrochemical activation of GC in 0.1 M KNO_3, a common supporting electrolyte used for graphite activation (2, 14). As can be seen in the STM image (Figure 1a), there is a significant change in the apparent surface roughness as a result of electrochemical treatment compared to the polished electrode (Figure 2a). The surface roughness apparent in Figure 1a is attributed to the presence of graphite oxide, resulting in topographical and electronic changes at the surface. At polished GC, defects that are a result of gas pockets formed during the fabrication process are also present (not shown), although their density is low (15). The surface roughness shown in Figure 1a is not as pronounced as that reported elsewhere (16). This is most likely due to a lower anodic overpotential used during our treatment. In contrast to the surface roughness apparent in STM images (Figure 1a), AFM images (Figure 1b) reveal a relatively smooth surface with isolated defects with diameters on the order of 100 nm. Although the relatively smooth surface seen by AFM may be a result of the tip dipping through the oxide layer, this is unlikely based on the STM images, which suggest an uneven distribution of oxide across the surface. Similar isolated defects as shown in Figure 1b were observed at different positions on the electrode surface.

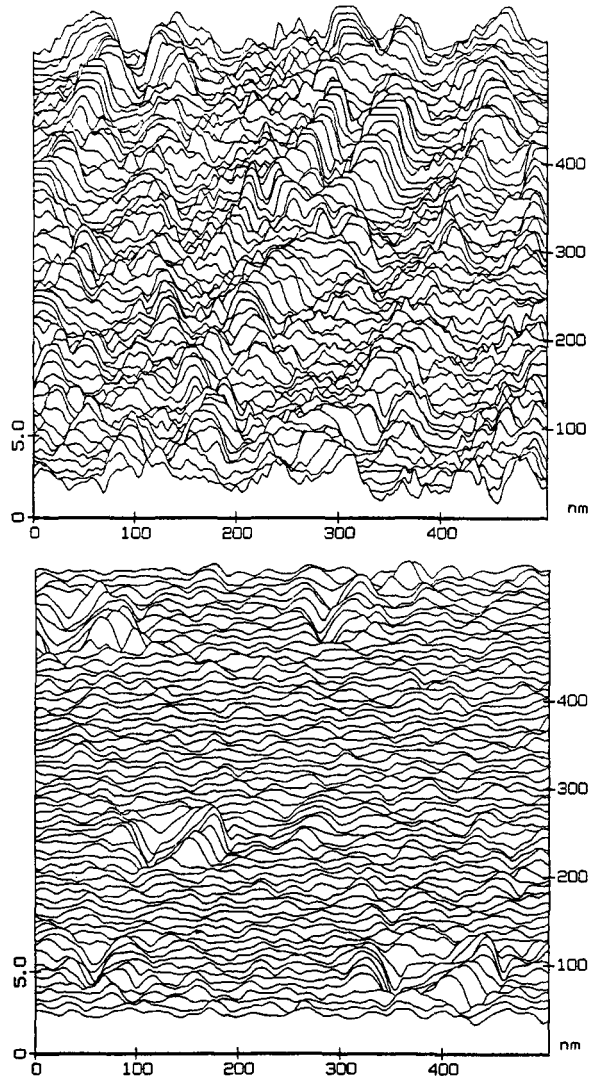

Figure 1. (a, top) Constant-current STM image (tip bias +100 mV, tunneling current 2 nA) and (b, bottom) constant-force AFM image (100-μm Si_3N_4 triangular cantilever, spring constant 0.58 N/m) of GC in air following electrochemical treatment in 0.1 M KNO_3. *XYZ* axis in nm.

Usually, at least one defect was observed in any given 500- × 500-nm field. It should be noted that larger, irregular-shaped defects, grooves, and much larger gas pockets were also observed, however not nearly as often. This is consistent with copper deposition patterns observed with SEM on electrochemically treated GC electrodes where copper nuclei with diameters on the order of 100 nm were separated by distances between 100 and 1000 nm and where such grooves were also observed (15). It has been suggested that a compacted microparticle layer is formed as a result of electrode polishing and that this layer is responsible for the less active nature of polished GC (15, 24). It is, therefore, possible that defect formation occurs at pinholes present in the compacted layer. This seems unlikely since changes in the diameter of pinholes with a distribution as seen by AFM (Figure 1b) would not significantly change the observed activity of the electrode.

Although it is not clear what mechanism controls the formation, size, and distribution of the observed defects, defects may ultimately control the electrode activity. Defects of similar diameter and shape have also been observed with STM on HOPG as a result of gasification reactions that result in the oxidation of graphite (27). The uniformity of the size and shape of the defects produced by gasification has been explained by the presence of atomic defects (i.e., edge sites) at

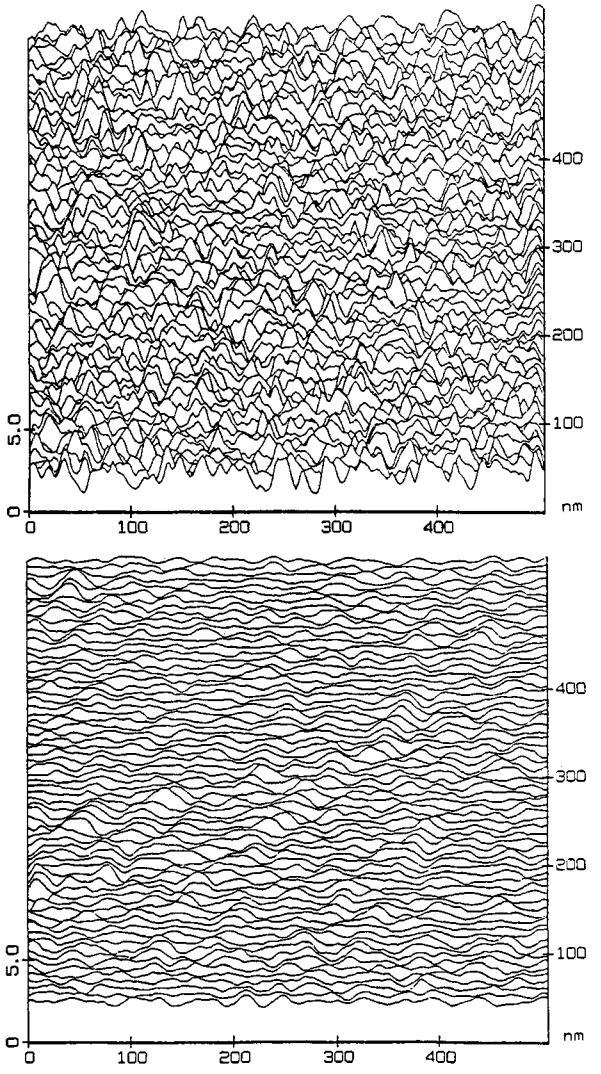

Figure 2. (a, top) Constant-current STM image (tip bias +100 mV, tunneling current 2 nA) and (b, bottom) constant-force AFM image (100-μm Si_3N_4 triangular cantilever, spring constant 0.58 N/m) of polished GC in air. *XYZ* axis in nm.

which the oxidation rate is significantly faster (27). Defects produced by different methods of oxidation (including gasification and electrooxidation) may form by the same mechanism.

Results similar to those at GC electrodes electrochemically treated in KNO_3 were obtained in phosphate buffer (pH 7) and H_2SO_4. In both cases, STM images showed an increase in apparent surface roughness as a result of treatment, while AFM images showed circular defects similar to those shown in Figure 1b. Treatment in KCl did not increase apparent surface roughness as imaged by STM. This is consistent with the fact that the oxidation of chloride (32) is the dominant anodic reaction, thereby decreasing the amount of oxide formation during treatment. Although defects were observed after electrochemical treatment in KCl, they were not as prevalent as on surfaces treated in the other supporting electrolytes.

In conclusion, it has been demonstrated that, except for the case of treatment in KCl, electrochemical treatment of GC results in an inhomogeneous surface, which is apparent from the changes in the STM tunneling current compared to that at polished electrodes. As a result, images obtained by STM show complicated topography. In this study, it has been shown that because of the nature of AFM, which is insensitive to electronic inhomogeneities, it can be used to show actual topographical information. This is critical in order to determine the surface structure of electrodes and ultimately their activity. Further work will include in situ STM and AFM imaging of reactions at the observed defects.

ACKNOWLEDGMENT

We thank Joseph Franek for useful discussions related to this work.

LITERATURE CITED

(1) Engstrom, R. C. *Anal. Chem.* **1982**, *54*, 2310–2314.
(2) Engstrom, R. C.; Strasser, V. A. *Anal. Chem.* **1984**, *56*, 136–141.
(3) Wightman, R. M.; Deakin, M. R.; Kovach, P. M.; Kuhr, W. G.; Stutts, K. J. *J. Electrochem. Soc.* **1984**, *131*, 1578–1583.
(4) Hu, I.; Karweik, D. H.; Kuwana, T. *J. Electroanal. Chem. Interfacial Electrochem.* **1985**, *188*, 59–72.
(5) Cabaniss, G. E.; Diamantis, A. A.; Murphy, W. R.; Linton, R. W.; Meyer, T. J. *J. Am. Chem. Soc.* **1985**, *107*, 1845–1853.
(6) Nagaoka, T.; Yoshino, T. *Anal. Chem.* **1986**, *58*, 1037–1042.
(7) Wang, J.; Tuzhi, P. *Anal. Chem.* **1986**, *58*, 1787–1790.
(8) Kovach, P. M.; Deakin, M. R.; Wightman, R. M. *J. Phys. Chem.* **1986**, *90*, 4612–4617.
(9) Nagaoka, T.; Yoshino, T. *Anal. Chem.* **1986**, *58*, 1953–1955.
(10) Wang, J.; Lin, M. S. *Anal. Chem.* **1988**, *60*, 499–502.
(11) Kepley, L. J.; Bard, A. J. *Anal. Chem.* **1988**, *60*, 1459–1467.
(12) Nagaoka, T.; Fukunaga, T.; Yoshino, T. *Anal. Chem.* **1988**, *60*, 2766–2769.
(13) Gewirth, A. A.; Bard, A. J. *J. Phys. Chem.* **1988**, *92*, 5563–5566.
(14) Bowling, R.; Packard, R. T.; McCreery, R. L. *Langmuir* **1989**, *5*, 683–688.
(15) Bodalbhai, L.; Brajter-Toth, A. *Anal. Chim. Acta* **1990**, *231*, 191–201.
(16) Wang, J.; Martinez, T.; Yaniv, D. R.; McCormick, L. D. *J. Electroanal. Chem. Interfacial Electrochem.* **1990**, *278*, 379–386.
(17) Smyrl, W. H.; Atanasoski, R. T.; Atanasoska, L.; Hartshorn, L.; Lien, M.; Nygren, K.; Fletcher, E. A. *J. Electroanal. Chem. Interfacial Electrochem.* **1989**, *264*, 301–304.
(18) Poon, M.; McCreery, R. L. *Anal. Chem.* **1986**, *58*, 2745–2750.
(19) Poon, M.; McCreery, R. L. *Anal. Chem.* **1988**, *60*, 1725–1730.
(20) Bowling, R. J.; Packard, R. T.; McCreery, R. L. *J. Am. Chem. Soc.* **1989**, *111*, 1217–1223.
(21) Sternitzke, K. D.; McCreery, R. L. *Anal. Chem.* **1990**, *62*, 1339–1344.
(22) Evans, J. F.; Kuwana, T. *Anal. Chem.* **1977**, *49*, 1632–1635.
(23) Stutts, K. L.; Kovach, P. M.; Kuhr, W. G.; Wightman, R. M. *Anal. Chem.* **1983**, *55*, 1632–1634.
(24) Kazee, B.; Weisshaar, D. E.; Kuwana, T. *Anal. Chem.* **1985**, *57*, 2736–2739.
(25) Fagan, D. T.; Hu, I. F.; Kuwana, T. *Anal. Chem.* **1985**, *57*, 2759–2763.
(26) Hu, I. F.; Kuwana, T. *Anal. Chem.* **1986**, *58*, 3235–3239.
(27) Chang, H.; Bard, A. J. *J. Am. Chem. Soc.* **1990**, *112*, 4598–4599.
(28) Binnig, G.; Rohrer, H. *IBM J. Res. Dev.* **1986**, *30*, 355–369.
(29) Binnig, G.; Quate, C. F.; Gerber, C. *Phys. Rev. Lett.* **1986**, *56*, 930–933.
(30) Albrecht, T. R.; Quate, C. F. *J. Appl. Phys.* **1987**, *62*, 2599–2602.
(31) Kinoshita, K. *Carbon: Electrochemical and Physicochemical Properties*; Wiley: New York, 1988; Chapter 6 and references therein.
(32) Beck, F.; Junge, H.; Krohn, H. *Electrochim. Acta* **1981**, *26*, 799–809.
(33) Maeda, Y.; Okemoto, Y.; Inagaki, M. *J. Electrochem. Soc.* **1985**, *132*, 2369–2372.
(34) Kinoshita, K. *Carbon: Electrochemical and Physicochemical Properties*; Wiley: New York, 1988; pp 210–211.

* Author to whom correspondence should be addressed.

Michael S. Freund
Anna Brajter-Toth*

Department of Chemistry
University of Florida
Gainesville, Florida 32611-2046

Therese M. Cotton

Department of Chemistry
Iowa State University
Ames, Iowa 50011

Eric R. Henderson

Department of Zoology and Genetics
Iowa State University
Ames, Iowa 50011

RECEIVED for review November 13, 1990. Accepted February 14, 1991. This work was supported, in part, by grants from the National Institutes of Health (Grant Nos. GM35341-03A2 ABT and GM35108 TMC) and the National Science Foundation (Grant No. DIR-9004649 ERH).